Machinery & Energetics
Vol. 13, No. 1. 2022

Journal homepage:
https://technicalscience.com.ua/en

UDC 621:664: 669.01(075)
DOI: 10.31548/machenergy.13(1).2022.26-33

Yevgen Aftandiliants[1*], Dainis Viesturs[2]

[1]National University of Life and Environmental Sciences of Ukraine
03041, 15 Heroiv Oborony, Kyiv, Ukraine

[2]Latvian University of Life Sciences
LV-3001, 2 Velika Str., Jelgava, Latvia

Oxidation processes of superalloys of the working layer and interfacial surfaces of bimetallic pairs

Abstract. Most superalloy steels, especially those alloyed with chromium, tungsten, cobalt, and molybdenum, are strongly riveted during plastic deformation by drawing. Superalloy steels with a clean, scale-free surface are susceptible to stick-slip with the carbide tool – drag. Therefore, in case of cold deformation, it is necessary to use special lubricants with extreme pressure components and strong lubricating coatings. After cleaning the surface from scale, a lime-salt coating is applied. Recently, a fairly effective sub-coating of the composition (in an aqueous solution) has been used: sodium sulphate Na_2SO_4 – 130…250 g/l; liquid glass Na_2SiO_3 – 20…30 g/l; treatment at a temperature of 80…90°C. In some technological processes, thin metal coatings are used as an oil coating – copper, lead-tin, and oxalate. After deformation, all types of coatings must be completely removed, since heat treatment can lead to processes of interaction of metal with lubricating coatings. This can lead to deterioration of the surface quality and loss of the necessary properties. The purpose of the study is to create a methodological framework for the oxidation processes of superalloys of the working layer and interfacial surfaces of bimetallic pairs. Methodology – thermodynamic calculations of the equilibrium of chemical reactions on the metal – gas phase interface surfaces. The paper presents the results of experimental studies with the established dependence of the isobaric potential on temperature for reactions on the interfacial surface "Me_2 – gas phase". The authors obtained the dependence of the isobaric potential on temperature for gaseous reaction products on the surface of superalloys. The existence of the dependence of the isobaric potential on temperature for reactions of the formation of complex oxides on the surface of superalloys is confirmed. Scientific significance – the adequacy of oxidation processes of superalloys of the working layer and interfacial surfaces of bimetallic pairs has been experimentally confirmed

Keywords: steel, alloys, chemical composition, oxides, interface surfaces, bimetallic castings

Article's History: Received: 11/10/2021; Revised: 14.01.2022; Accepted: 23.02.2022

INTRODUCTION

The production of high-quality bimetallic castings is possible only if a high-quality connection of the working layer with the base is formed [1].

The development of a high-quality technological process for the production of bimetallic castings makes it necessary to conduct a complex of research measures to investigate the features of their development [2]. The main purpose of this stage is to investigate the oxidation processes of steels and alloys of the main and working layers and determine the chemical composition of simple and complex oxides on the base, working layer, and interfacial surfaces [3].

A reliable diffusion bond between alloys belonging to bimetallic pairs can be obtained after studying the oxidation processes of superalloys of the working layer and calculating the composition of complex oxides on interfacial surfaces [4].

Therefore, the problem of investigating the features of oxidation processes of superalloy working layers and calculating the composition of complex oxides on interfacial surfaces is urgent.

Investigations of the oxidation processes of carbon, low-alloy steels and superalloys belonging to bimetallic pairs, and the content of complex oxides, were carried

Suggested Citation:
Aftandiliants, Ye., & Viesturs, D. (2022). Oxidation processes of superalloys of the working layer and interfacial surfaces of bimetallic pairs. *Machinery & Energetics,* 13(1), 26-33.

*Corresponding author

out using the method of thermodynamic calculations of the equilibrium of chemical reactions on the surfaces of the metal-gas phase interface [5]. The main advantage of thermodynamic research methods is the possibility of conducting a theoretical analysis of the oxidation process without its preliminary experimental implementation [6]. A special feature of the method is the preliminary systematisation of not only the temperature functions of the logarithm equation of the equilibrium constant K_r, but also the functions of the enthalpy ΔH, changes in the entropy ΔS, and changes in the thermal coefficients of the heat capacities of all participants in the reaction ΔCp [7]. The values of the logarithms of the reaction equilibrium constant are calculated according to the equation given in [8].

$$IgK_r = \frac{\Delta f(\Delta H)}{T} + \Delta f(\Delta S) + \Delta C_0 \cdot M_0 + \\ + \Delta C_1 \cdot M_1 + \Delta C_2 \cdot M_2 + \Delta C_{-2} \cdot M_{-2} \quad (1)$$

where T – temperature, K; M_0, M_1, M_2, M_{-2} – temperature functions; ΔC_0, ΔC_1, ΔC_2, ΔC_{-2} – heat capacity coefficients.

To assess the possibility of implementing the studied reactions, the isobaric potential was determined at a given temperature in [9]:

$$\Delta Z_T^0 = -4{,}575 \cdot T \cdot 1\ell gK_r \quad (2)$$

The composition of complex oxides on interfacial surfaces was studied by x-ray phase analysis on a DR-2 x-ray diffractometer [10]. Samples of cylindrical alloys with a diameter of 20 mm and a height of 15 mm oxidised at a temperature of 1,000°C with an exposure time of 30 hours were used as the object of research [11]. Diffraction spectra were obtained in monochromatic Cukl – radiation [12]. A single graphite crystal placed on a diffracted beam was used as a monochromator [13].

This shooting geometry allows reducing the fluorescent background and recording the diffraction spectra of iron-based alloys in copper radiation [14]. Diffragrams were obtained by step scanning in the range of angles 2θ from 10 to 90° [15]. The scanning step was 0.05°, and the exposure time was 3-5 seconds. The scanning speed was 0.5°/min. Data processing of the diffractometric experiment was performed using a program for full-profile analysis of x-ray spectra from a mixture of polycrystalline phase components powder cell 2.4 [16].

During the calculation process, the periods of elementary cells of phase components [17], the half-width of x-ray profiles [18], the background line [19], and the mass fractions of phases [20] were specified.

The purpose of the study is to create a methodological framework for the oxidation processes of superalloys of the working layer and interfacial surfaces of bimetallic pairs.

RESULTS AND DISCUSSION

To investigate the processes of oxide formation on the surfaces of superalloys of the working layer of bimetallic castings, thermodynamic calculations of possible oxidation reactions at the interfacial boundaries "Me_2 – gas phase" in the temperature range of 1,100-1,700 K were performed.

On the surface of superalloys 240x16 (12% Cr – ASTM A532 Class II Type A), 300x12g5 (300 Cr12Mn5 – marking of Ukraine) and 260x28 (25% Cr-ASTM A532 Class III Type A), oxidation of iron, carbon, silicon, manganese, chromium, sulphur, and phosphorus is possible. Reactions of interaction of iron and manganese with sulphur with the generation of iron and manganese sulphides are also possible. Oxidation of iron, silicon, manganese, and chromium is carried out by reactions (3)-(9).

$$Fe + ½O_2 \rightarrow FeO, \quad (3)$$
$$4Fe + 3O_2 \rightarrow Fe_2O_3, \quad (4)$$
$$3Fe + 2O_2 \rightarrow Fe_3O_4, \quad (5)$$
$$[Si]_{0.36} + O_2 \rightarrow SiO_2, \quad (6)$$
$$[Mn]_{0,65} + O_2 \rightarrow MnO, \quad (7)$$
$$3[Mn]_{0,65} + 2O_2 \rightarrow Mn_3O_4, \quad (8)$$
$$4[Cr]_{0,3} + 3O_2 \rightarrow 2Cr_2O_3. \quad (9)$$

The formation of sulphides corresponds to reactions (10) and (11).

$$Fe + [S] \rightarrow FeS, \quad (10)$$
$$[Mn] + [S] \rightarrow MnS. \quad (11)$$

On the surface of superalloys, the formation of a complex oxide $MnSiO_3$ is possible by reaction:

$$[Mn] + [Si] + \frac{3}{2O_2} \rightarrow MnSiO_3, \quad (12)$$

superalloys 300X12M (GJN-HV600 (XCR11 – EN – JN3019), 300X12G3M (300Cr12Mp3Mo – marking of Ukraine), 300X12G5M (300Cr12Mp5Mo – marking of Ukraine), 300X20M2 (GJN-HV600 (XCr18) –EN-JN3039) are oxidised and form oxides of iron, silicon, manganese, and chromium on the surface by reactions (3)-(9), and iron and manganese sulphides can be formed by reactions (10) and (11). The reaction (13) of Mo oxidation to MoO_3 is added to the above:

$$2[Mo] + 3[O_2] \rightarrow MoO_3. \quad (13)$$

Alloy 300x22 (20% Cr-Mo – ASTM A532 Class II Type D) in addition to the main elements such as iron, carbon, silicon, manganese, and chromium contains vanadium and titanium. The following oxidation reactions of these elements were studied:

$$4[V] + 3O_2 \rightarrow 2V_2O_3, \quad (14)$$
$$[V] + O_2 \rightarrow VO_2(\beta), \quad (15)$$
$$2[V] + 2O_2 \rightarrow V_2O_4(\beta), \quad (16)$$
$$Ti + O_2 \rightarrow TiO_2(rutile), \quad (17)$$
$$2Ti + 3/2O_2 \rightarrow Ti_2O_3. \quad (18)$$

On the surface of the alloy 300X16M2 (GJN-HV600 (XCr14) – EN-JN3029), oxidation of elements by reactions (3)-(12), and oxidation of copper to CuO and Cu_2O oxides is possible:

$$[Cu] + ½O_2 \rightarrow Cuo, \quad (19)$$
$$[Cu] + ½O_2 \rightarrow Cu_2O. \quad (20)$$

On the surface of a superalloy 350XH2 (GJN-HV550 – EN-JN2029), oxidation by reactions is possible (3)-(9), (12), and the formation of sulphides by reactions (10) and (11). To these reactions, it is necessary to add the nickel oxidation reaction to NiO:

$$NiT + ½O_2 \rightarrow NiO, \quad (21)$$

Dependence of the isobaric potential on temperature for reactions on the interfacial surface "Me_2 – gas phase" is shown in Figure 1.

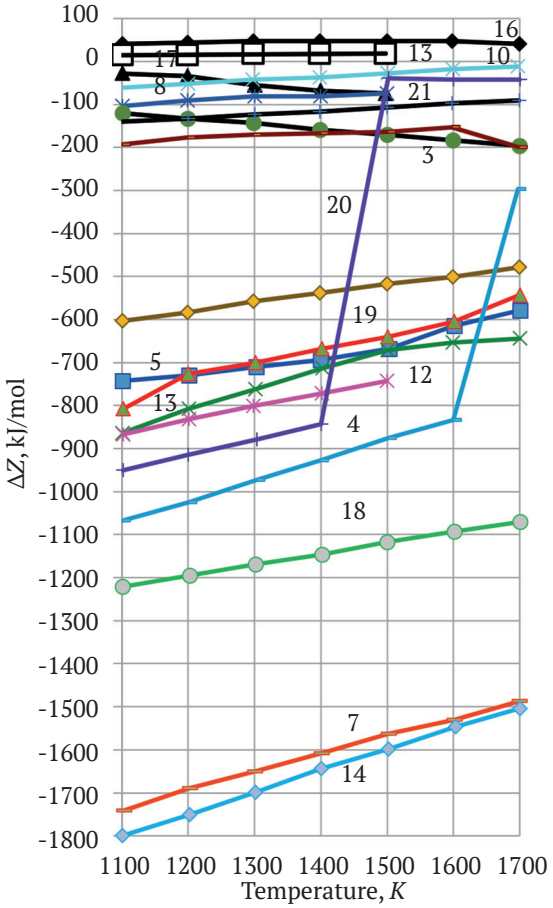

Figure 2. Dependence of the isobaric potential on temperature for reactions on the interfacial surface "Me_2 – gas phase"

The most likely reactions for superalloys are 240x16 (12% Cr – ASTM A532 Class II Type A), 300X12G5 (300 $Cr_{12}Mn_5$ – marking of Ukraine) and 260x28 (25% Cr – ASTM A532 Class III Type A) there are reactions (9) – oxidation of chromium to Cr_2O_3, reaction (4) oxidation of iron to hematite at temperatures below 1,600 K, reaction (8) oxidation of manganese to Mn_3O_4 at temperatures of 1,400 K and below, and reaction (12) – oxidation of manganese and silicon to form a complex oxide $MnSiO_3$ at temperatures below 1,500 K.

At temperatures of 1,500-1,700 K, the reaction (16) is unlikely, and in the range of 1,400-1,500 K, the isobaric potential drops sharply. The reactions (13) and (18) are less likely – oxidation of iron to magnetite and oxidation of silicon to SiO_2 reaction (7) – oxidation of manganese to MPO. The following are unlikely: reaction (3) – oxidation of iron to visstite, reaction (11) – formation of manganese sulphide, and reaction (10) – formation of iron sulphide.

For superalloys 300X12M (GJN-HV600 (XCR11) – EN-JN3019), 300X12G3M (300$Cr_{12}Mn_3Mo$ – marking of Ukraine), 300 $Sg_{12}Mn_5Mo$ – marking of Ukraine) and 300X20M2 (GJN-HV600 (XCr18) – EN-JN3039) to the reactions discussed above, the reaction (13) – oxidation of molybdenum to MoO_3 is added, which is most likely, and the isobaric potential decreases in this temperature range with $\Delta Z_{1,700}$=-577 kJ mol to $\Delta Z_{1,100}$=-863 kJ/mol.

On the surface of a superalloy 300X22 (20% Cr-Mo-ASTM A532 Class II Type D) to reactions (3)-(9), (10) and (11) the reactions (14)-(16) – vanadium oxidation and reactions (17), (18) – titanium oxidation are added.

Thermodynamic calculation of reactions (14)-(16) vanadium oxidation revealed that reaction (14) – vanadium oxidation to V_2O_5, is the most likely: $\Delta Z_{1,700}$=-1,491 kJ/mol, $\Delta Z_{1,100}$=-1,801 kJ/mol. Reactions (15) and (16) are impossible, since their isobaric potential is a positive value. Reactions (17) and (18) – oxidation of titanium to TiO_2 and Ti_2O_3, accordingly, they are the most likely and with a decrease in temperature the potential decreases: $\Delta Z_{1,700}$=-1,066 kJ/mol, $\Delta Z_{1,100}$=-1,218 kJ/mol of reaction (16), a $\Delta Z_{1,700}$=-642 kJ/mol and $\Delta Z_{1,100}$=-746 kJ/mol – for reaction (17).

On the surface of a superalloy 300X16M2 (GJN – HV600 (XCr14) - EN-JN3029), reactions (3)-(12) are added to reactions (19) and (20) – oxidation of copper to CuO and Cu_2O. Both of these reactions are the least likely: $\Delta Z \approx$-12÷-98 kJ/mol.

On the surface of a superalloy 350XH2 (GJN-HV550 – (EN-JN2029) to reactions (3)-(9), (10)-(12) added reaction (21) – oxidation of nickel to NiO_t oxide. Based on the value of the isobaric potential, it can be assumed that it is unlikely, $\Delta Z \approx$-90÷-142 kJ/mol.

When superalloys are oxidised, gaseous reaction products are also formed: CO_2, CS_2, COS, SO, SO_2, SiO, and PO. Figure 2 shows the dependence of the isobaric potential in the range of 1,100-1,700 K reactions (22)-(28) – the formation of gaseous products.

$$[C]O_2 \rightarrow C2\uparrow, \quad (22)$$

$$[C]+2[S] \rightarrow CS_2\uparrow, \quad (23)$$

$$[C]+[S]+½O_2 \rightarrow COS\uparrow, \quad (24)$$

$$[S]+½O_2 \rightarrow SO\uparrow, \quad (25)$$

$$[S]+O_2 \rightarrow SO_2\uparrow, \quad (26)$$

$$[Si]+½O_2 \rightarrow SiO\uparrow, \quad (27)$$

$$[P]+½O_2 \rightarrow PO\uparrow. \quad (28)$$

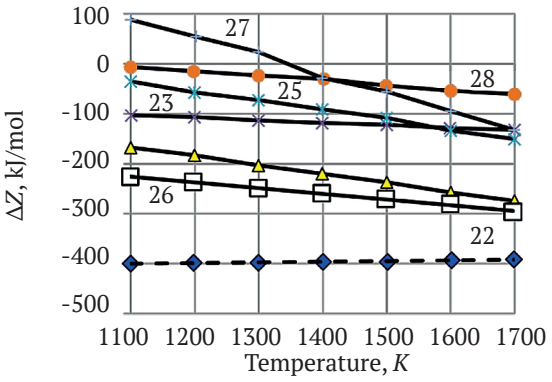

Figure 2. Dependence of the isobaric potential on temperature for gaseous reaction products on the surface of superalloys

The most likely reaction is (22) – carbon oxidation to $CO_2\uparrow$. Reactions (26) and (24) – formation of SO2 and COS are less likely. Reactions (25), (27), and (28) – formation of SO, SiO, and PO, respectively, are less likely. Reaction (21) – formation of CS_2 in the range of 1,350-1,700 K is less likely, and at temperatures below 1,350 K it is impossible.

The superalloys listed above have their own number of most likely oxidation reactions. Figure 3 shows a histogram for superalloys.

For superalloys 240X16 (12% Cr – ASTM A532 Class II Type A), 300x12g5 (300 Cr12Mn5 – marking of Ukraine), 260x28 (25% Cr-ASTM A532 Class III Type A), a number of reaction probabilities are presented in Table 1.

For superalloys 300X12M (GJNHV600 (XCr11) – EN-JN3019), 300X12G3M (300Cr12Mn3Mo – marking of Ukraine), 300X12G5M (300Cr12Mn5Mo – marking of Ukraine) and 300X20M2 (GJN – HV600 (XCr18) – EN-JN3039) a number of probabilities are shown in Table 2.

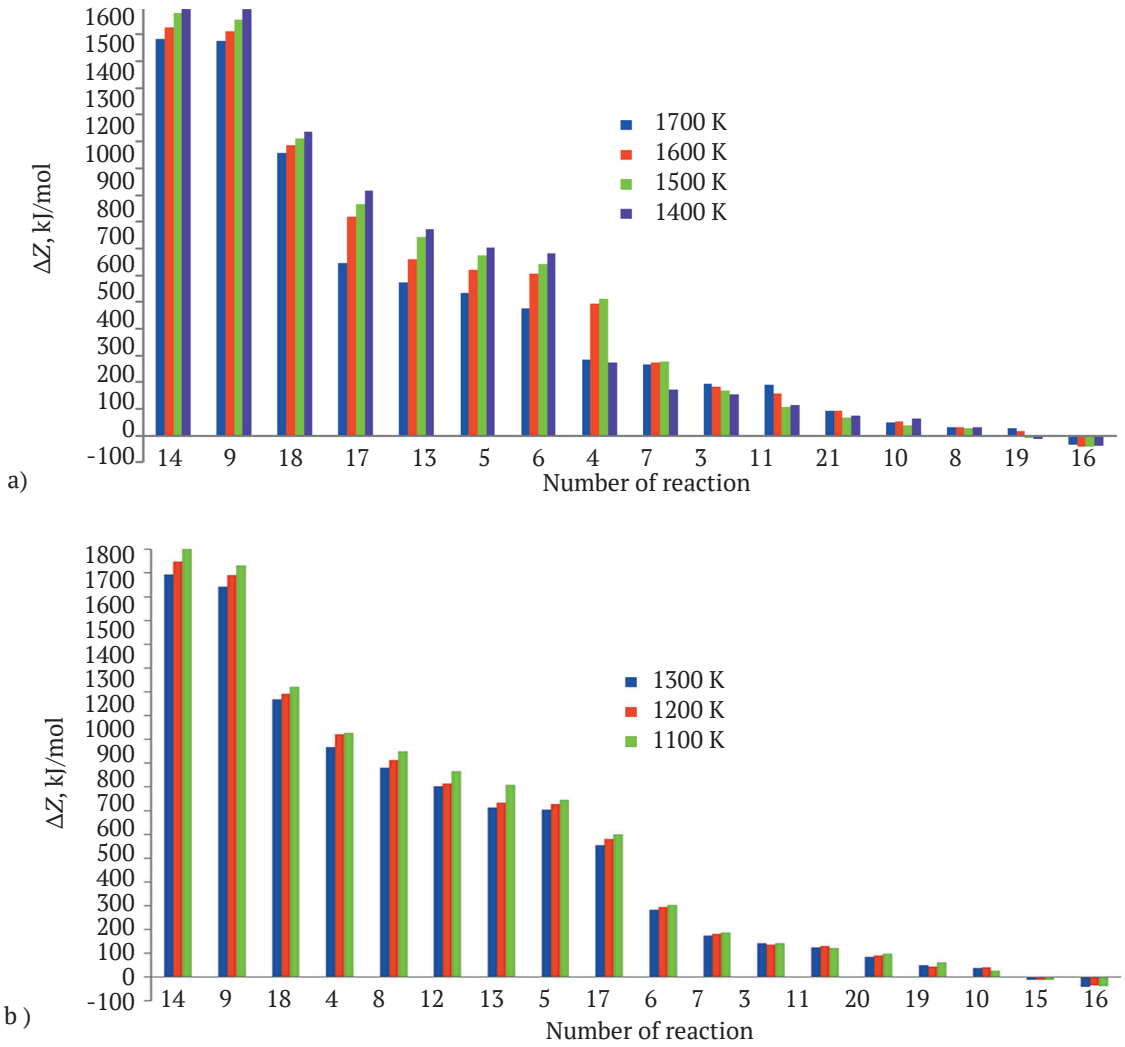

Figure 3. Dependence of the isobaric potential on temperature for solid-phase products on superalloys: a) temperature range from 1,400 to 1,700 K; b) 1,100 to 1,300 K

Table 1. A number of probabilities of oxidation reactions and formation of iron and manganese sulphides on superalloys 240X16 (12% Cr – ASTM A532 Class II Type A), 300x12g5 (300 Cr12Mn5 – marking of Ukraine), 260x28 (25% Cr-ASTM A532 Class III Type A)

T, K	Number of reaction probabilities									
1.700	9	5	6	4	7	3	11	10	8	–
1.600	9	4	5	6	7	11	3	10	8	–
1.500	9	4	12	5	6	7	11	3	10	8
1.400	9	4	8	12	5	6	7	3	11	10
1.300	9	4	8	12	5	6	7	3	11	10
1.200	9	4	8	12	5	6	7	3	11	10
1.100	9	4	8	12	5	6	7	3	11	10

Table 2. A number of probabilities of oxidation reactions and formation of iron and manganese sulphides on superalloys 300X12M (GJN – HV600 (XCr11) – EN-JN3019), 300X12G3M (300Cr12Mn3Mo – marking of Ukraine), 300X12G5M (300Cr12Mn5Mo – marking of Ukraine) and 300X20M2 (GJN – HV600 (XCr18) – EN-JN3039)

Temperature, K						
1.100	1.200	1.300	1.400	1.500	1.600	1.700
Number of reaction probabilities						
9	9	9	9	9	9	9
4	4	4	4	4	4	13
8	8	8	8	12	13	5
12	12	12	12	13	5	6
13	13	13	13	5	6	4
5	5	5	5	6	7	7
6	6	6	6	7	11	3
7	7	7	7	11	3	11
3	3	3	3	3	10	10
11	11	11	11	10	8	8
10	10	10	10	8	–	–

A number of probabilities for a superalloy 300x22 (20% Cr-Mo – ASTM A532 Class II Type D) are presented in Table 3.

Table 3. A number of probabilities of oxidation reactions and formation of iron and manganese sulphides on a superalloy 300x22 (20% Cr-Mo – ASTM A532 Class II Type D)

Temperature, K						
1,100	1,200	1,300	1,400	1,500	1,600	1,700
Number of reaction probabilities						
14	14	14	14	14	14	14
9	9	9	9	9	9	9
18	18	18	18	18	18	18
4	4	4	4	4	4	17
8	8	8	8	12	17	5
12	12	12	12	17	5	6
5	5	17	17	5	6	4
17	17	5	5	6	7	7
6	6	6	6	7	11	3
7	7	7	7	11	3	11
3	3	3	3	3	10	10
11	11	11	11	10	8	8
10	10	10	10	8	14	16
14	14	14	14	14	16	–
16	16	16	16	16	–	–

For a superalloy 300X16M2 (GJNHV600 (XCr14) – EN-JN3029), a number of probabilities are presented in Table 4.

Table 4. A number of probabilities of oxidation reactions and formation of iron and manganese sulphides on a superalloy 300X16M2 (GJN-HV600 (XCr14) – EN-JN3029)

Temperature, K						
1.100	1.200	1.300	1.400	1.500	1.600	1.700
Number of reaction probabilities						
9	9	9	9	9	9	9
4	4	4	4	4	4	13
8	8	8	8	12	13	5
12	12	12	12	13	5	6
13	13	13	13	5	6	4
5	5	5	5	6	7	7
6	6	6	6	7	11	3
7	7	7	7	11	3	11
3	3	3	3	3	10	10
11	11	11	11	20	8	8
20	20	20	20	10	15	19
19	19	10	10	19	16	16
10	10	19	19	8	-	-
15	15	15	15	15	-	-
16	16	16	16	16	-	-

A number of probabilities on a superalloy 350XH2 alloy (GJN-HV550 – EN-JN2029) are presented in Table 5.

Table 5. A number of probabilities of oxidation reactions and formation of iron and manganese sulfides on a superalloy 350XH2 (GJNHV550 – EN-JN2029)

Temperature, K						
1,100	1,200	1,300	1,400	1,500	1,600	1,700
Number of reaction probabilities						
9	9	9	9	9	9	9
4	4	4	4	4	4	5
8	8	8	8	12	5	6
5	5	5	5	6	7	7
12	12	12	12	5	6	4
5	5	5	5	6	7	7
6	6	6	6	7	11	3
7	7	7	7	11	3	11
3	3	3	3	3	21	21
21	21	11	11	21	10	10
11	11	21	21	10	8	8
10	10	10	10	8	-	-

Figure 2 shows a histogram of gaseous reaction products on the surface of superalloys.

A number of probabilities of possible gaseous reaction products are shown in Table 6.

Table 6. A number of probabilities of gaseous products of oxidation reactions at the interfacial boundary "Me_2 – gas phase"

T, K	Number of reaction probabilities						
1,700	22	26	24	25	27	23	28
1,600	22	26	24	25	27	23	28
1,500	22	26	24	27	25	23	28
1,400	22	26	24	27	25	28	23
1,300	22	26	23	27	25	28	23
1,200	22	26	24	27	25	28	23
1,100	22	26	24	27	25	28	22

Oxides formed on the surface of superalloys can interact with each other to form complex oxides by reactions:

$$FeO + Cr_2O_3 \rightarrow FeO \cdot Cr_2O3, \quad (29)$$

$$MnO + SiO_2 \rightarrow MnSiO_3, \quad (30)$$

$$FeO + SiO_2 \rightarrow FeO \cdot SiO_2. \quad (31)$$

To determine the possibility formation of complex oxides on the surfaces of alloys 300X12M (GJN-HV600 (XCr11) – EN-JN3019), 300X12G3M (300Cr12Mn3Mo – marking of Ukraine), 300X12G5 (300 Cr12Mn5 – marking of Ukraine), 300X16M2 (GJN-HV600 (XCr14) – EN-JN3029), 300X20M2 (GJNHV600 (XCr18) – EN-JN3039) thermodynamic calculation of the isobaric potential of these reactions of complex oxide formation in the range of 1,100-1,800 K is performed.

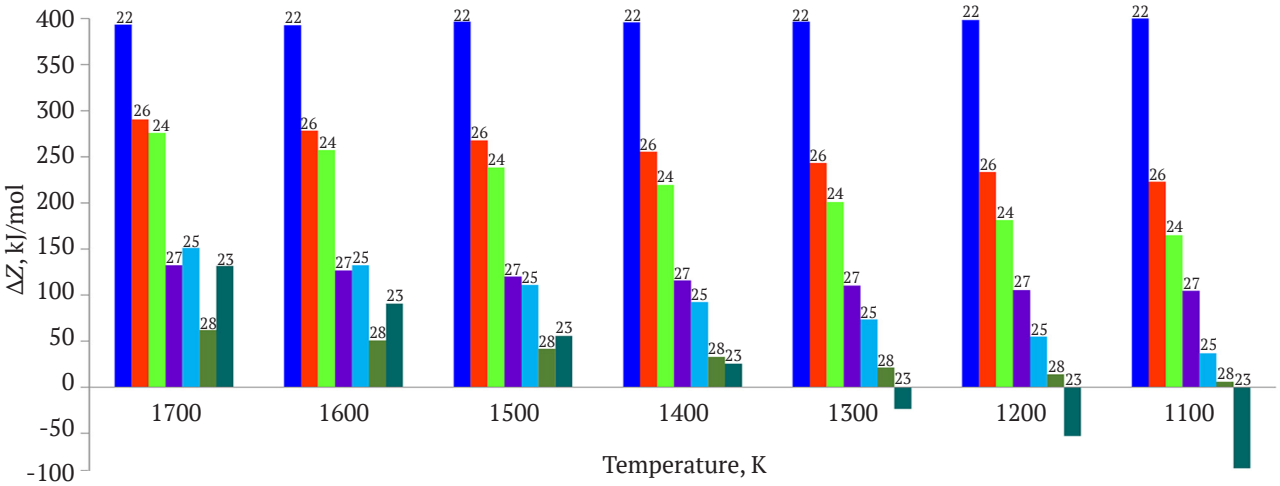

Figure 3. Dependence of the isobaric potential on superalloys

The dependence of the isobaric potential on temperature for complex oxide formation reactions is shown in Figure 5.

Calculations show that the following complex oxides can form on the surface of superalloys: $FeO \cdot Cr_2O_3$, $MnO \cdot SiO_2$ and $2FeO \cdot SiO_2$. The most likely reaction is (29) – the formation of a complex oxide $FeO \cdot Cr_2O_3$. Reactions (30) and (31) – formation of complex oxides $MnO \cdot Sio_2$ and $2FeO \cdot SiO_2$ – accordingly, they are unlikely due to their small size ΔZ. Reaction (31) at temperatures of 1,700-1,800 K is not possible.

In order to study the phase composition of complex oxides, an x-ray phase analysis of oxide films formed on the surface of superalloys was performed.

The results of x-ray phase analysis are presented in Table 7.

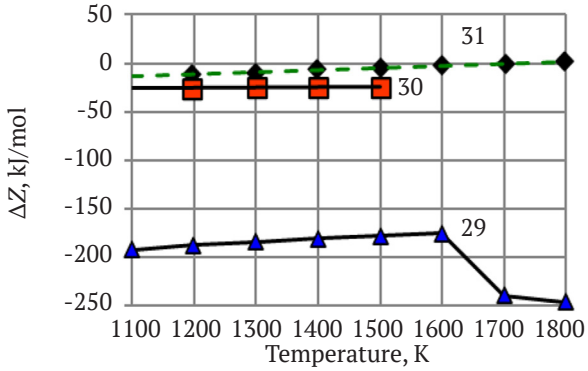

Figure 5. Dependence of the isobaric potential on temperature for reactions of formation of complex oxides on the surface of superalloys

Table 7. Results of studying the phase composition of oxide films on superalloys

Object of research	Phase composition
300X12M GJN-HV600 (XCr11) (EN-JN3019)	Fe_2O_3 (rhombohedral lattice); Fe_2O_3 (cube); Cr_2O_3; $Fe_2O_3 \cdot Mn_2O_3$; $Cr_2O_3 \cdot Fe_2O_3$
300X12G3M 300Cr12Mn3Mo	Fe_2O_3 (rhombohedron); Fe_2O_3 (cube); $Cr_2O_3 \cdot FeO$; $Cr_2O_3 \cdot Fe_2O_3$; $Fe_2O_3 \cdot Mn_2O_3$; $Cr_2O_3 \cdot 3Fe_2O_3$
300X12G5 300Cr12Mn5	γ- Fe; α- Fe; Fe_2O_3 (rhombohedron); Fe_2O_3 (cube); $Fe_2O_3 \cdot Cr_2O_3$; $Fe_2O_3 \cdot Mn_2O_3$
300X16M2 GJN-HV600 (XCr14) (EN-JN3029)	α- Fe; γ- Fe; Fe_2O_3 (rhombohedron); Fe_2O_3 (cube); Fe_3O_4; $Fe_2O_3 \cdot Mn_2O_3$; $Cr_2O_3 \cdot 3Fe_2O_3$
300X20M2 GJN-HV600 (XCr18) (EN-JN3039)	α- Fe; γ- Fe; Fe_2O_3 (rhombohedron); Fe_2O_3 (cube); Fe_3O_4; $Mn_2O_3 \cdot Fe_2O_3$; $Cr_2O_3 \cdot Fe_2O_3$

The results of the x-ray phase study showed that complex oxides are formed on all superalloys. The largest amount of complex oxides is formed on the alloy 300x12G3M (300$Cr_{12}Mn_3Mo$ – marking of Ukraine): Cr_2O_3·FeO; Cr_2O_3·Fe_2O_3; Fe_2O_3·Mn_2O_3; Cr_2O_3·3Fe_2O_3. Superalloys 300X12M (GJN-HV600 (XCr_{11}) – EN-JN3019), 300X12G5 (300 $Cr_{12}Mn_5$ – marking of Ukraine) and 300X20M2 (GJN-HV600 (XCr_{18}) – EN-JN3039) form two complex oxides Fe_2O_3 each. Mn_2O_3 and Cr_2O_3 Fe_2O_3. Complex oxides Fe_2O_3 are formed on the 300x16M2 alloy. Mn_2O_3 and Cr_2O_3·3Fe_2O_3. Presence of complex oxide Cr_2O_3·FeO and lack of MnO·SiO2 and 2FeO·SiO_2 in oxide films confirm the results of the performed thermodynamic calculations.

CONCLUSIONS

1. It is established that on the surfaces of superalloys of the working layer in the temperature range of 1,700-1,100 K as a result of oxidation reactions, the following solid-phase oxides are formed: FeO, Fe_2O_3, Fe_3O_4, SiO_2, MnO, Mn_3O_4, $MnSiO_3$, Cr_2O_3, MoO_3, V_2O_3, TiO_2 (rutile), Ti_2O_3, Sio, Cu_2O, NiO. As gaseous products of reactions, Co_2, SS_2, COS, SO, SO_2, SiO, PO are formed.

2. It is established that complex oxides are formed on the surfaces of superalloys due to oxidation reactions: Cr_2O_3·FeO, Cr_2O_3·3Fe_2O_3, 3Cr_2O_3·2Fe_2O_3, Cr_2O_3·Fe_2O_3, Fe_2O_3·Mn_2O_3.

REFERENCES

[1] Wróbel, T. (2014). Characterization of bimetallic castings with an austenitic working surface layer and an unalloyed cast steel base. *Journal of Materials Engineering and Performance*, 23(5), 1711-1717.

[2] Eivani, A.R., & Karimi Taheri, A. (2007). A new method for producing bimetallic rods. *Materials Letters*, 61(19-20), 4110-4113.

[3] Kizu, T., Nagataki, Y., Inazumi, T., & Hosoya, Y. (2001). Effects of chemical composition and oxidation temperature on the adhesion of scale in plain carbon steels. *ISIJ International*, 41(12), 1494-1501.

[4] Lavrishchev, A.V., Prokopev, S.V., & Tynchenko, V.S. (2021). Investigation of the solid-phase joint of VT-14 titanium alloy with 12KH18N10T stainless steel obtained by diffusion welding through intermediate layers. *Metals*, 11(8), number article 1325.

[5] Zhang, H.L., Huang, P.Z., Sun, J., & Gao, H. (2004). Morphological healing evolution of penny-shaped fatigue microcracks in pure ironat elevated temperatures. *Applied Physics Letters*, 85, 1143-1145.

[6] Göbl, M., Eder, H., Prestl, A., Siller, I., & Schnitzer, R. (2020). Diffusion bonding of high-alloyed tool steels with maraging and precip-itation hardening steels. *Metals*, 10, number article 1622.

[7] Aftandiliants, Y., & Gnyloskurenko, S. (2021). Development of advanced alloy steels for machinery. *Engineering for Rural Development*, 20, 706-711.

[8] Du, J., Wang, H., & Zhao, R. (2013). Size-dependent thermodynamic properties and equilibrium constant of chemical reaction in nanosystem: an experimental study (II). *The Journal of Chemical Thermodynamics*, 65, 29-33.

[9] Rogovskii, I.L., Titova, L.L., Voinash, S.A., Melnyk, V.I., Remshev, E.Yu., Galiyev, G.R., Nuretdinov, D.I., & Vornacheva, I.V. (2021). Design of landing of assembly machine building units with circulating load rolling bearing rings. *Journal of Physics*, 1889, number article 042004.

[10] Yang, L., Haber, J.A. Armstrong, Z., & Yang, S.J. (2021). Discovery of complex oxides via automated experiments and data science. *Proceedings of the National Academy of Sciences*, 118(37), number article e2106042118.

[11] Behrens, B.-A., Brunotte, K., Peddinghaus, J., & Heymann, A. (2022). Influence of dwell time and pressure on SPS process with titanium aluminides. *Metals*, 12(1), number article 83.

[12] Nazarenko, I., Mishchuk, Y., Mishchuk, D., Ruchynskyi, M., Rogovskii, I., Mikhailova, L., Titova, L., Berezovyi, M., & Shatrov, R. (2021). Determiantion of energy characteristics of material destruction in the crushing chamber of the vibration crusher. *Eastern-European Journal of Enterprise Technologies*, 4(7(112), number article 49.

[13] Veklich, A., Tmenova, T., Zazimko, O., Trach, V., Lopatko, K., Titova, L., Boretskij, V., Aftandiliants, Y., Lopatko, S., & Rogovskiy, I. (2020). Regulation of biological processes with complexions of metals produced by underwater spark discharge. *Springer Proceedings in Physics. Nanostructure Surfaces, and Their Applications*, 247, 283-306.

[14] Lutz, J., & Pernicka, E. (2007). Energy dispersive X-ray fluorescence analysis of ancient copper alloys: Empirical values for precision and accuracy. *Archaeometry*, 38(2), 313-323.

[15] Mukhametzyanov, T., Fatkhutdinova, A., & Schick, C. (2022). Step-scan differential calorimetry of protein denaturation: Modeling and experiment. *Thermochimica Acta*, 710, number article 179181.

[16] Rogovskii, I.L., Titova, L.L., Voinash, S.A., Sokolova, V.A., Pushkov, Yu.L., Krivonogova, A.S., & Kokieva, G.E. (2020). Modeling the distribution of internal stresses in surface strengthened layer of steel parts after cementation and hardening. *Journal of Physics: Conference Series*, 1679, number article 042069.

[17] Wang, Y., Zhou, B., Zhao, R., Wang, B., Liu, Q., & Dai, M. (2022). Super-accuracy calculation for the half width of a voigt profile. *Mathematics*, 10, number article 210.

[18] Chausov, M., Brezinova, J., Pylypenko, A., Maruschak, P., Titova, L., & Guzanova. A. (2019). Modification of mechanical properties of high-strength titanium alloys VT23 and VT23m due to impact-oscillatory loading. *Metals*, 9(80), 2-18.

[19] Mahar, A., Wang, P., Ali, A., Awasthi, M.K., Lahori, A.H., & Wang, Q. (2020). Challenges and opportunities in the phytoremediation of heavy metals contaminated soils: A review. *Ecotoxicol Environ Saf*, 126, 111-121.

[20] Abdallah, A., Reichel, E., Heinisch, M., & Jacoby, B. (2021). Symmetric plate resonators for viscosity and density measurement. *Procedia Engineering*, 87, 36-39.

Євген Григорович Афтанділянц[1], Дайніс Віастурс[2]

[1]Національний університет біоресурсів і природокористування України
03041, вул. Героїв Оборони, 15, м. Київ, Україна

[2]Латвійський університет наук про життя
LV-3001, вул. Velika, 2, м. Єлгава, Латвія

Процеси окислення високолегованих сплавів робочого шару і міжфазних поверхонь біметалевих пар

Анотація. Більшість високолегованих сталей, особливо легованих хромом, вольфрамом, кобальтом, молібденом, сильно наклепуються при пластичній деформації волочінням. Високолеговані сталі з чистою поверхнею без окалини схильні до схоплювання-налипання з твердосплавним інструментом – волоками. Тому при холодній деформації необхідно застосовувати спеціальні мастила з протизадирними компонентами та міцні підмастильні покриття. Після очищення поверхні від окалини наносять вапняно-сольове покриття. Останнім часом почали застосовувати досить ефективне підмастильне покриття складу (у водному розчині): сульфат натрію Na_2SO_4 – 130…250 г/л; рідке скло Na_2SiO_3 – 20…30 г/л; обробка при температурі 80…90 °С. В окремих технологічних процесах використовують як підмастильні покриття металеві тонкі покриття – мідні, свинцево-олов'яні, а також оксалатне. Після деформації всі види покриттів повинні бути повністю видалені, так як при термообробці можуть протікати процеси взаємодії металу зі змащувальними покриттями. Це може призвести до погіршення якості поверхні та втрати необхідних властивостей. Мета статті – створення методологічного апарату процесів окислення високолегованих сплавів робочого шару і міжфазних поверхонь біметалевих пар. Методологія – термодинамічні розрахунки рівноваги хімічних реакцій на поверхнях розділу "метал – газова фаза". В статті представлено результати експериментальних досліджень із встановлена залежність ізобарного потенціалу від температури для реакцій на міжфазній поверхні "Me2 – газова фаза". Авторами отримана залежність ізобарного потенціалу від температури для газоподібних продуктів реакцій на поверхні високолегованих сплавів. Підтверджено існування залежності ізобарного потенціалу від температури для реакцій утворення комплексних оксидів на поверхні високолегованих сплавів. Наукова значимість – експериментальним шляхом підтверджена адекватність процесів окислення високолегованих сплавів робочого шару і міжфазних поверхонь біметалевих пар

Ключові слова: сталь, сплави, хімічний склад, оксиди, поверхні розділу, біметалеві виливки